

# Digital Computer Application in the F-15 Engine Air Inlet Control System

C.J. Scherz\* and L.E. Williams†  
*McDonnell Douglas Corporation, St. Louis, Mo.*

The F-15 is a high-performance air superiority fighter capable of speeds in excess of Mach 2.5. Trade studies showed that an inlet with three variable compression ramps and a variable capture area feature would enhance overall weapon system performance. The control mechanism that was chosen for positioning the inlet variable surfaces is presented. A study showed that a serial digital computer mechanization for the air inlet controller Air Inlet Controller (AIC) was preferred over an analog or parallel digital computer mechanization. The details of the production digital AIC are described. The accuracy and dynamic response requirements of the AIC were determined by simulation and other studies. Extensive ground tests and a wind-tunnel test verified the excellent operation of the digital AIC. Several AIC reprogrammings were required during the ground, wind-tunnel, and flight testing in order to optimize the aircraft performance. These were easily accomplished due to the digital mechanization. Flight test results show that the inlet control system and the AIC have adequate steady-state accuracy and dynamic response characteristics for control of the inlet system to provide excellent performance and low inlet distortion during extreme aircraft maneuvers.

## Nomenclature

$I$	= actuator drive current
$M$	= Mach number
$P$	= pressure
$T$	= total temperature
$X$	= actuator extension
$\alpha$	= aircraft angle of attack
$\Delta$	= angle with respect to the reference line in the rotating structure
$\rho$	= angle of first ramp with respect to aircraft water line (defined to be +7 deg when the inlet reference line is parallel to the aircraft water line)

## Subscripts

$B$	= bypass door
$0$	= freestream probe static for pressure, freestream for Mach number
$P$	= probe
$ST$	= inlet throat static
$TO$	= freestream probe pitot for pressure, freestream for temperature
$TT$	= inlet throat probe pitot
$1$	= first ramp
1 SCHEDULE	= scheduled first ramp
3	= third ramp
3 SCHEDULE	= scheduled third ramp
4	= diffuser ramp

## Introduction

THE two F-15 engine air inlets are two dimensional with three overhead horizontal compression ramps and a variable capture area feature. The inlets must provide airflow

Presented as Paper 77-1480 at the AIAA 2nd Digital Avionics Systems Conference, Los Angeles, Calif., Nov. 2-4, 1977; submitted Nov. 22, 1977; revision received March 13, 1978. Copyright © American Institute of Aeronautics and Astronautics, Inc., 1977. All rights reserved.

Index categories: Guidance and Control; Computer Technology; Airbreathing Propulsion.

\*Section Chief, Guidance and Control Mechanics, Engineering Technology Division, McDonnell Aircraft Co.

†Lead Engineer, Guidance and Control Mechanics, Engineering Technology Division, McDonnell Aircraft Co.

to the engines with low inlet total pressure distortion to preclude distortion induced stalls, and must operate with high total pressure recovery and low spillage drag to enhance aircraft performance.

Studies prior to the development phase of the F-15 propulsion system indicated that an engine air inlet which was controlled as a function of Mach number, freestream total temperature, and angle of attack would significantly enhance the performance of the F-15.

The reliability, weight, ease of schedule change, maintenance, in-flight and ground built-in testing (BIT), and accuracy requirements of the AIC could only have been met by the use of the digital computer mechanization.

The excellent performance of the AIC is evidenced by the superb performance of the F-15 itself during both the flight testing and in-service operation of the more than 200 F-15s delivered to the Air Force.

## F-15 Engine Air Inlet

The F-15 engine air inlet, shown in Fig. 1, is a two-dimensional horizontal three-ramp, external compression design with partially cut-back sideplates. For high supersonic operation, compression is accomplished through three oblique shocks and a terminal normal shock. The capture area varies as a function of Mach number, angle of attack, and temperature through rotation of the three forward ramps. A throat slot bleed system also acts as a bypass system for

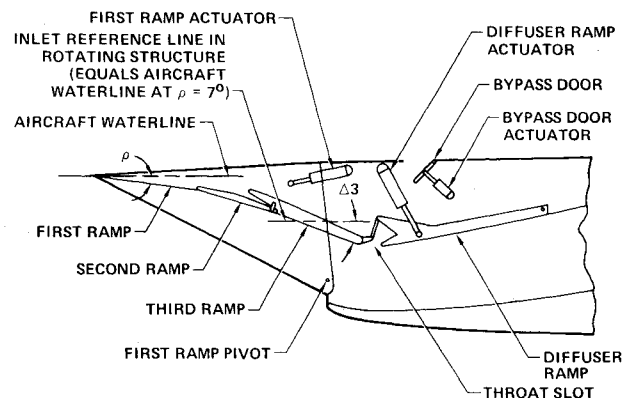


Fig. 1 Inlet ramp mechanism.

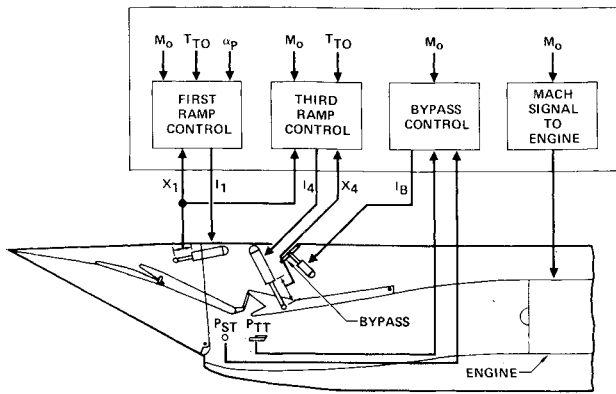


Fig. 2 Inlet control system.

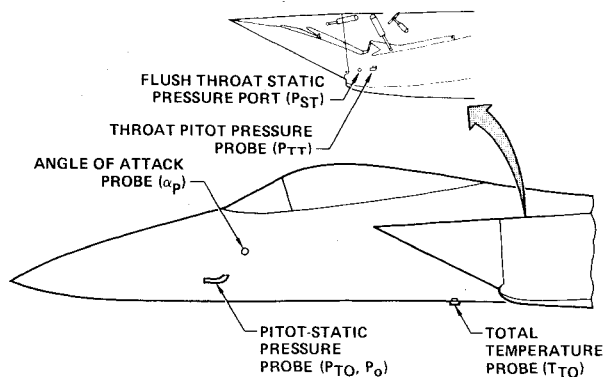


Fig. 3 Inlet control system sensors.

inlet/engine airflow matching. Details of the inlet and the studies leading to the selection of the inlet configuration are presented by Sams<sup>1</sup> and Imfeld.<sup>2</sup>

### Inlet Control System

A simplified schematic of the F-15 inlet control system is shown in Fig. 2. The inlet control system was designed to satisfy a number of requirements including thrust, drag, distortion, structural airloads, and aircraft stability. The ramp angles and the rotational position of the inlet are set as a function of freestream Mach number, angle of attack, and total temperature to produce the required inlet pressure recovery and to match the engine airflow requirements for standard and nonstandard day conditions. The inlet is rotated to maintain constant local angle of attack until the rotation limits are reached, to reduce aircraft drag, and to provide low-inlet pressure distortion and turbulence in maneuvers. The bypass door is positioned as a function of freestream and duct Mach numbers to accommodate, as necessary, the airflow variation caused by the engine, inlet and control system tolerances, and reduced engine airflows at supersonic, high-altitude flight conditions.

### Inlet Control System Sensors

The inlet control system sensors are shown in Fig. 3. The sensors are duplicated on the other side of the aircraft. The freestream Mach number is sensed by an L-probe pitot-static probe on the side of the aircraft. The reading of this probe varies with angle of attack because of flow variations caused by the aircraft forebody. The AIC must have a compensation map for the angle-of-attack effects. As shown in Fig. 2, the compensated  $M_0$  signal is sent to the engine electronic control for use in the engine control schedules.

### First Ramp Control System

The first ramp control system is designed to position the first ramp angle,  $\rho$ , as a function of Mach number, angle of

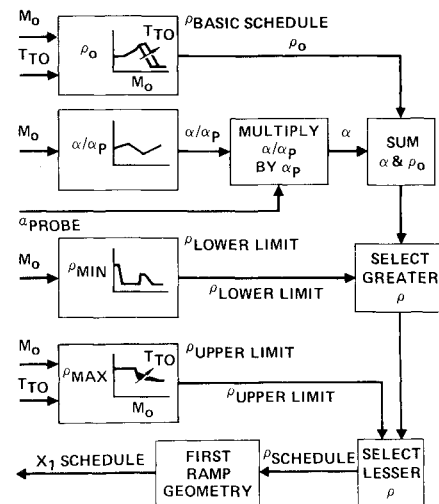


Fig. 4 First ramp schedule.

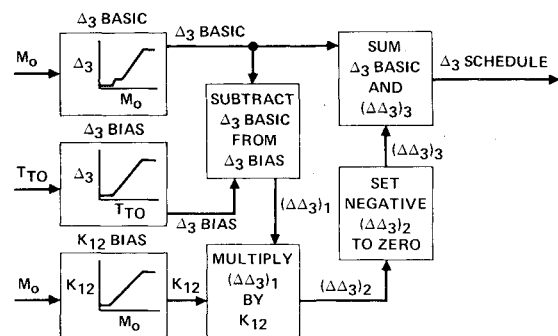


Fig. 5 Third ramp schedule.

attack, and total temperature. The first ramp angle is defined in Fig. 1. The scheduled value of  $\rho$  is a compromise which maximizes thrust minus drag while providing acceptable distortion.<sup>1-3</sup> It is also shown by Mello<sup>3</sup> that the first ramp rotation adds up to 1%  $\hat{c}$  static stability to the aircraft handling qualities. This saves 180 lb, compared to other methods of providing the same stability. Rotating the ramps also maintains the airloads constant on the first ramp, since the airstream hits the ramp at the same angle until the rotational limits are reached. This also provides a weight saving since the ramp backup structure can be reduced.

The first ramp control system is mechanized to control the first ramp actuator extension  $X_1$ , shown in Fig. 2.  $X_1$  is proportional to  $\rho$ . The desired  $X_1$  is computed as a function of  $M_0$ ,  $\alpha_p$ , and  $T_{TO}$ . The difference signal between the desired  $X_1$  and the actual  $X_1$  is used to move the first ramp actuator to minimize the error.

The schedule for the first ramp, or  $\rho$ , is shown in Fig. 4. The  $\rho_{\text{BASIC SCHEDULE}}$  is a function of  $M_0$  and  $T_{TO}$ . The  $\rho_0$  angle corresponds to  $\alpha_p$  equal to zero. As shown in Fig. 4, the scheduled rotation is simply the sum of the rotation angle at 0 deg angle of attack plus the angle of attack within the upper and lower scheduled limits. The lower limit is a function of  $M_0$ , while the upper limit is a function of  $M_0$  and  $T_{TO}$ . The scheduled rotation is converted to a scheduled position of the first ramp actuator  $X_{1\text{SCHEDULE}}$ .

### Third Ramp Control System

The purpose of the third ramp control system is to control the angle  $\Delta_3$  shown in Fig. 1. The  $\Delta_3$  angle is measured between the third ramp surface and a reference line in the variable cowl. The line is parallel to the aircraft waterline when the cowl is at  $\rho = 7$  deg.

The method used to develop the  $\Delta_3$  schedule is described by Sams<sup>1</sup> and Imfeld.<sup>2</sup> The  $\Delta_3$  angle is controlled by the diffuser

ramp actuator shown in Fig. 1. The third ramp control, shown schematically in Fig. 2, computes a scheduled value of  $\Delta_3$ , based on the measured  $M_0$  and  $T_{TO}$ . The third ramp angle  $\Delta_3$  is a function of the first ramp actuator extension  $X_1$  and the diffuser ramp actuator extension  $X_4$ . From the measured value of  $X_1$  and the scheduled  $\Delta_3$ , a scheduled value of  $X_4$  is computed from a stored geometry map. The difference between the scheduled value of  $X_4$  and the measured value of  $X_4$  is used to move the diffuser ramp actuator to minimize the error between the desired and measured  $X_4$ s.

The third ramp schedule is shown in Fig. 5. The  $\Delta_{3BASIC}$  schedule is a function of  $M_0$ . It is the controlling schedule below Mach 1.0. Above Mach 1.2, the scheduled value of  $\Delta_3$  is the larger of  $\Delta_{3BASIC}$  or  $\Delta_{3BIAS}$ . The quantity  $\Delta_{3BIAS}$  is a function of  $T_{TO}$ . The  $K_{I2BIAS}$  schedule is provided to gradually incorporate the effect of  $\Delta_{3BIAS}$  between Mach 1.0 and 1.2.

The movable second ramp is mechanically connected between the first and third ramps.

#### Bypass Control System

The purpose of the bypass control system is to control the Mach number at the throat of the inlet by movement of the bypass door shown in Fig. 1. There is an aerodynamic coupling between the bypass door and the throat Mach number. The rationale used to determine the desired throat Mach number is described by Imfeld.<sup>2</sup> The desired throat Mach number is a function of  $M_0$ , as indicated in Fig. 2. The ratio of the static pressure  $P_{ST}$  measured in the throat and the pitot pressure  $P_{TT}$  measured in the throat, is a measure of the throat Mach number. The AIC causes the bypass door to move in order to minimize the difference between the measured  $P_{ST}/P_{TT}$  and the desired  $P_{ST}/P_{TT}$ .

#### Control System Dynamic Response Requirements

During the concept definition phase of the F-15 development, a simulation of the control system was developed to determine the control system dynamic response requirements. The simulation included dynamic models of the following components: 1)  $\alpha$  sensor; 2)  $P_0$ ,  $P_{TO}$  sensors and pneumatic lines; 3)  $P_{ST}$ ,  $P_{TT}$  sensors and pneumatic lines; 4)  $T_{TO}$  sensor; 5) first ramp, diffuser ramp, and bypass door actuators; 6) a simple aerodynamic model of the duct and bypass volume; and 7) inlet geometry relations.

The engine airflow demand was represented by a scheduled flow as a function of  $T_{TO}$  and by transfer functions.

The simulation was subjected to various input transients, including representations of: aircraft acceleration (Mach number change); angle-of-attack changes corresponding to aircraft maneuvers; longitudinal gusts; shock wave caused by passing aircraft; and engine airflow transients corresponding to throttle bursts and chops.

From this study, it was determined that the high rate of angle-of-attack change due to aircraft maneuvers specified the control dynamic requirements. The angle-of-attack signal commands the first ramp actuator extension  $X_1$ , as shown in Fig. 4. The resultant high first ramp actuator velocity commands a high diffuser ramp actuator velocity through the  $X_4$  scheduling map. The bypass control must compensate for the rapid changes of  $X_1$  and  $\Delta_3$ .

The rates of response for the control systems were chosen so that control system response characteristics did not cause the inlet to operate supercritically or in buzz or near these regions of operation. Supercritical inlet operation or inlet operation in buzz causes high inlet distortion and a low level of inlet pressure recovery. The allowable ramp and throat pressure ratio dynamic errors are dependent on the flight condition, aircraft angle of attack, and ramp position. The allowable errors must be determined for each flight condition. The rate capabilities and dynamics of the control system components were varied in the simulation for several flight conditions until the inlet buzz and supercritical criteria were

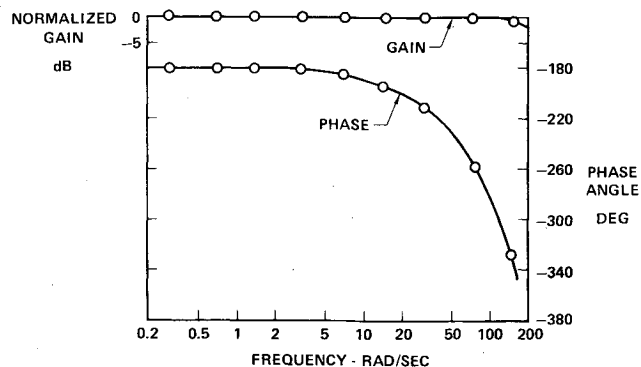


Fig. 6 First ramp controller normalized frequency response  $I_1/X_1$ .

satisfied. Simultaneously, linearized control system stability studies were performed to insure that each control system had 45 deg of phase margin and 6 dB of gain margin. This provides a stability margin for the variation in system characteristics.

It should be noted that for positive  $\alpha$  changes, the airloads on the first ramp increase as the actuator lags behind the command position. If the error gets too large, the airloads can stall the actuator and further increase the error, causing degraded inlet operation.

Based on these studies, the actuator rate limits were specified to be a minimum of: first ramp actuator:  $\pm 35$  deg/s; diffuser ramp actuator: 10 in./s; and bypass door actuator: 13 in./s.

The normalized frequency response characteristics of the first ramp portion of the AIC are shown in Fig. 6. The response characteristics are similar for the diffuser ramp and bypass portions of the AIC.

#### Control System Steady-State Accuracy Requirements

The control system schedule requirements were developed to satisfy a number of requirements, including thrust, drag, distortion, structural airloads, and aircraft stability. There are variations in all of the system components. If these variations get too large, the system performance will be unacceptable. The allowable errors vary with flight condition, but the nominal limits set on the inlet control system steady-state accuracies were first ramp-0.61 deg of  $\rho$  and third ramp-0.44 deg of  $\Delta_3$ . These errors were apportioned among the system components. The errors apportioned for the inlet controller were dependent on the slope of the control system schedule at the flight condition of interest.

#### Air Inlet Controller Computer Trade Study

A detailed tradeoff study showed that a serial digital computer was the best implementation for the F-15 AIC electronics. The three alternatives considered were serial digital, parallel digital, and analog computers.

The study is summarized in Table 1. Each comparison category is given a weighting proportional to its importance. It is evident from this summary that the serial digital approach, with a score of 97 out of a possible 100, is superior to the parallel digital and analog concepts, with scores of 91 and 61, respectively.

All three concepts that were considered would require essentially equivalent complexity for the input/output interface circuitry. These items were not considered in the study which concentrated on the type of processing/memory concept to be utilized.

#### Digital Electronic AIC Mechanization

The AIC schematic diagram is shown in Fig. 7. The basic task for this AIC mechanization consists of: 1) input interface—sensing and interfacing with inlet control and

Fig. 7 AIC schematic.

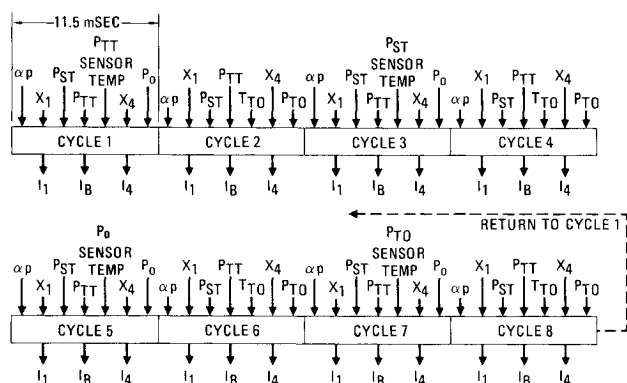
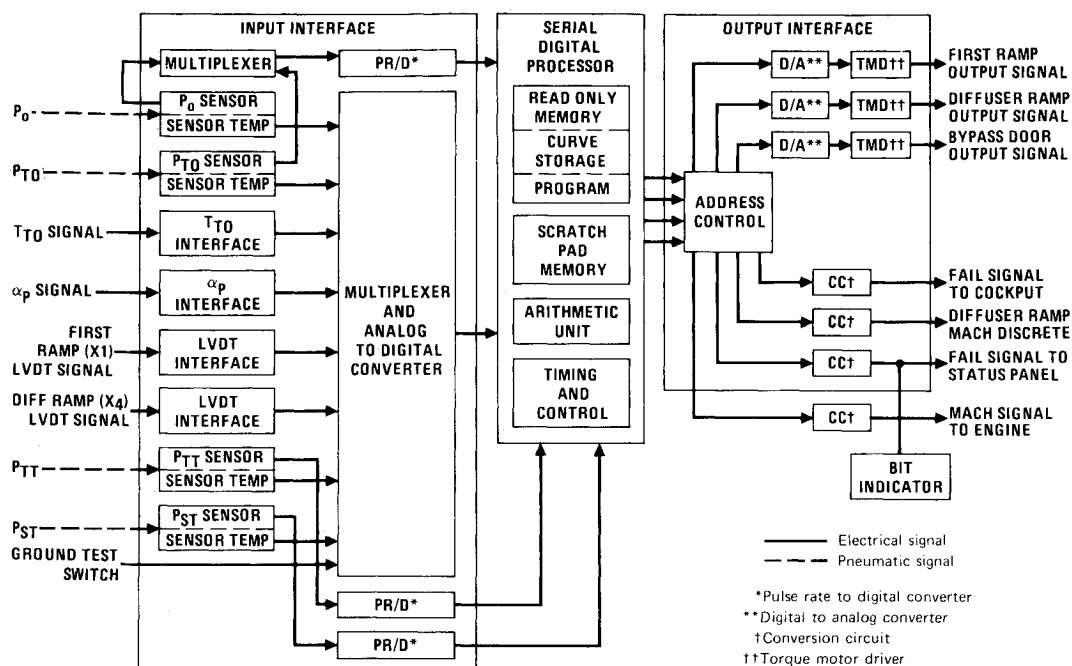


Fig. 8 AIC timing diagram.

freestream parameters; 2) serial digital processor — computation of the scheduled inlet configuration; 3) output interfacing with other aircraft equipment to achieve the scheduled inlet configuration; and 4) BIT provisions, both automatic and ground test.

#### Input Interface

The input interface is shown in Fig. 7. The sensed parameters are summarized in Table 2. The input interface consists of the basic electrical analog circuitry for each input plus two multiplexers, three pulse rate-to-digital converters, and an A/D converter.

A multiplexer is an electronic implementation of a switch which connects various inputs to a single processor in some computer-controlled sequence. The required signal processing hardware is obviously reduced by this time-sharing approach. The  $P_0$  and  $P_{T0}$  signals utilize the same 16-bit pulse rate-to-digital (PR/D) converter by virtue of a multiplexer. The inlet throat pressure signals ( $P_{ST}$  and  $P_{TT}$ ) require separate PR/D converters, since they must be updated more frequently. The remaining nine input signals utilize the same 12-bit A/D converter by virtue of a multiplexer. Table 3 lists the update time intervals for all the input and output signals, except the BIT failure signal which is discussed later in this section. The timing diagram in Fig. 8 shows the relative update times for the AIC inputs and outputs. The fastest update interval is 1 computer cycle. The slowest update interval is 8 computer cycles.

Table 1 Processor tradeoff ratings

Item	Maximum scores	Serial digital	Parallel digital	Analog
Accuracy				
Circuit limitations	5	5	5	2
Steady state	10	10	10	5
Long-term stability	10	10	10	5
Reliability				
Parts count	10	10	7	5
Parts usage history	5	5	5	4
No. of connections	5	4	3	4
Speed of response	15	13	15	15
Maintainability				
Extent of self-test	10	10	10	5
Periodic trimming	5	5	5	2
Flexibility				
Program changes	5	5	5	2
Schedule changes	3	3	3	1
Additional functions	2	2	2	1
Maintenance costs	10	10	8	7
Power requirement	5	5	3	3
Total	100	97	91	61

The pressure sensors are integral parts of the AIC. They have an allowable error band of only 0.03% of full scale for all error sources. The input pressure is sensed by the variation it produces in the natural frequency of a vibrating metal cylinder. An electrical pulse rate is generated corresponding to this frequency. The four pulse rates are converted to digital numbers by the PR/D converters. Each pressure is calculated in the digital processor as a nonlinear preprogrammed function of the corresponding pulse rate. Sensor temperature compensation is implemented in the digital processor and a correction is applied to each measured pressure.

#### Serial Digital Processor

The AIC serial digital computer processes data from the sensors and interface signals, calculates the scheduled inlet configuration, and calculates the appropriate drive signals to the actuators. Calculations are also made for a Mach number trim signal to the engine, detection of inlet buzz or supercritical operation, and detection of control system failures. The processor, shown in Fig. 7, is a serial digital

Table 2 AIC sensed parameters

Input parameter	Detected by
Local Mach number at aircraft freestream pressure probes	Static and pitot pressure sensors
Inlet throat Mach number	Static and pitot pressure sensors
Local angle of attack (AOA) at aircraft AOA sensor	Potentiometer on aircraft angle-of-attack sensor
Local total temperature at aircraft temperature probe	Aircraft temperature probe
First ramp actuator extension	Actuator linear variable differential transformer (LVDT)
Diffuser ramp actuator extension	Actuator LVDT

Table 3 A/D and D/A conversion intervals

Parameter	Input sampling interval		
	11.5 ms	23.0 ms	92.0 ms
Angle of attack	×		
First ramp extension	×		
Diffuser ramp extension	×		
Throat static pressure	×		
Throat pitot pressure	×		
Freestream static pressure		×	
Freestream pitot pressure		×	
Freestream total temperature		×	
Freestream static pressure sensor		×	
Freestream pitot pressure sensor			×
Throat static pressure sensor			×
Throat pitot pressure sensor			×
Parameter	Output conversion interval		
	11.5 ms		
First ramp servovalve current		×	
Diffuser ramp servovalve current		×	
Bypass door servovalve current		×	
Digital output			
Electronic engine control (12-bit serial word)		×	

mechanization of the following functions: 1) read only memory for schedule storage and program instruction; 2) scratch pad memory for temporary storage of computations; 3) arithmetic unit for computations; 4) multiplexers consisting of switching circuits for time sharing of processing among the various signals; 5) timing and control for sequencing and coordinating computer functions; and 6) power supply for accurate voltage and current control.

The AIC processor basic characteristics are: 1) basic word size is 16 bits, including sign; 2) computer iteration rate is 11.5 ms; 3) the basic computer clock rate is 2 Mhz with 4  $\mu$ s word time; 4) read-only MOS memory size is 1024 words including data storage plus instructions; 5) scratch pad memory consists of thirty-two 16-bit registers.

The input interface outputs from the three PR/D converters, plus the nine outputs from the A/D converter, plus the four pressure sensor compensation signals are multiplexed to facilitate use by the serial digital processor.

#### Output Interface

The output interface performs the conversion, formatting, and outputting of processor data. The processor output data streams are directed to the engine electronic control output

Table 4 AIC output interface

Hardware	AIC output interface
Ramp 1 servomotor	AIC input to servovalve
Diffuser ramp servomotor	AIC input to servovalve Discrete signal to indicate Mach > 1.5
Bypass servomotor	AIC input to servovalve
Cockpit warning light	Buzz detection Supercritical detection AIC built-in test (BIT) detected failure
Engine electronic control	Computed digital freestream Mach number AIC clock
Avionics status panel and LRU failure indicator	Bit detected AIC failure

stage, to the BIT interface, or to the D/A converters for conversion to analog drive signals to the servomotors. The AIC output interfaces are shown in Table 4.

The three actuator drive circuits (first ramp, third ramp, and bypass door) are identical, and each has a 10-bit D/A converter and a servovalve driver circuit. The engine electronic control signals are transmitted in a digital format. A BIT system output word is transmitted through a series-to-parallel converter to the AIC test connector to supply information for fault isolation to the card level. The BIT system also transmits a 28 V signal to the appropriate fault indicators upon detecting a failure. A discrete signal is sent to the diffuser ramp actuator as an indicator of whether the Mach number is greater or less than 1.5. Above Mach 1.5, a fail-safe feature in the diffuser actuator is activated, locking the actuator in position in the event of certain failures.

#### Analyses During the Development Phase of the F-15

As the characteristics of the control system components were chosen and the components were developed, the simulation of the inlet, inlet control system, and engine was continuously updated.

The AIC model was updated to include the dynamics of the interfaces with the system sensors and the actuator torque motors. The quantization effects of the A/D and D/A converters were simulated. The computation delays and various input and output sampling rates were also simulated. The AIC control system schedules were simulated, including the same reading and interpolation routines that are used in the AIC.

The actuator characteristics were also updated to include such effects as the torque motor dynamics and position limits and the second-stage spool dynamics and position limits.

Worst-case transients that occurred during combat maneuvers performed by pilots in the MCAIR F-15 Manned Air Combat Simulator Facility were used as transient inputs to the simulation.

The simulation was used to insure that the dynamic rate capabilities of the components were adequate. It was shown that the AIC basic 16-bit word size and the granularity of the A/D and D/A converters provided sufficient accuracy and smoothness of response. The AIC iteration rate was chosen to be 11.5 ms. The studies showed a performance degradation when the iteration rate was increased to 20 ms.

#### System Ground and Wind-Tunnel Testing

The thorough ground and wind-tunnel testing that was performed on the inlet control system, and some of the problems encountered and solved during the testing, are discussed in this section.

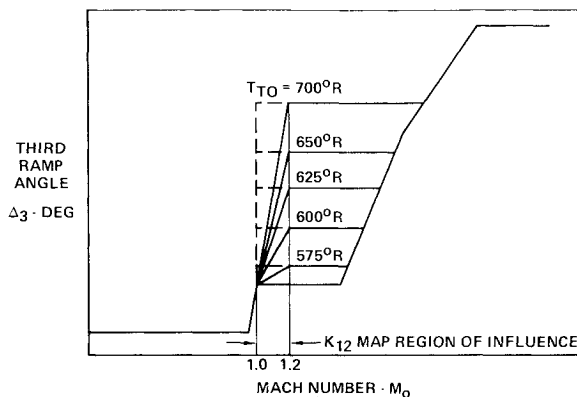


Fig. 9 Third ramp schedule biasing.

#### Inlet Controller Stability and Performance Test

During the development phase of the F-15, the inlet control system was tested using a mechanical test setup which duplicated the inertias of the moving parts of the inlet. The spring rates of the ramps and actuators were also simulated. Flightworthy actuators were installed in the setup. Both a breadboard and a prototype AIC were used in the testing. Pneumatic supplies were provided for  $P_{TO}$ ,  $P_0$ , and  $P_{TT}$ . The bypass control loop was closed by means of an analog computer and a pneumatic function generator connected between the bypass door and the  $P_{ST}$  input to the AIC. The analog computer simulated the bypass duct aerodynamic transfer function. The function generator was also used to provide dynamic inputs of  $P_{TO}$  and  $P_0$ .

The correct steady-state operation of the system was verified. The system was subjected to simulated  $\alpha$  inputs, Mach number transients, gusts, and other pneumatic transients. The testing indicated that some changes had to be made in the AIC program.

#### Freestream Pressure Ratio Filtering

As shown in Fig. 8, the freestream pitot pressure  $P_{TO}$  and the freestream static pressure  $P_0$  are sampled on alternate 11.5 ms cycles. The AIC computes the ratio of  $P_{TO}$  to  $P_0$  for use as the Mach number input to the AIC schedules. During a constant Mach number climb,  $P_{TO}$  and  $P_0$  are decreasing, but the ratio stays constant. However, the computed ratio does not stay constant because of the alternate cycle sampling. A ripple therefore developed in the  $P_{TO}/P_0$  signal, which caused the first and diffuser ramps to chatter. The solution to this problem was to filter the  $P_{TO}/P_0$  signal with a digital first-order lag which had a 0.1 s time constant. The AIC was reprogrammed to add the filter.

#### Third Ramp Control Schedule Modifications

The third ramp control schedules were presented in Fig. 5. The Fig. 5 schedules represent the AIC program at the end of the inlet controller stability and performance test. The program did not have the  $K_{12BIAS}$  schedule before the test. Figure 9 shows the combined effects of the  $\Delta_{3BASIC}$  and  $\Delta_{3BIAS}$  schedules. The dashed lines correspond to the schedule before the test; the sloping schedule lines (added during the test) correspond to the Fig. 5 schedules. With the original schedule, when the Mach number was increased past Mach 1.0 and  $T_{TO}$  was 700°R, there was an abrupt 8 deg increase in  $\Delta_3$  which was unacceptable. The addition of the  $K_{12BIAS}$  allowed a smooth transition between the  $M_0$  and  $T_{TO}$  schedules. The AIC was reprogrammed to include the  $K_{12BIAS}$ . The capability of the AIC to allow rapid reprogramming of the control system allowed the testing to be completed in a timely fashion.

#### Full-Scale Inlet/Engine Compatibility Test

A full-scale model of the F-15 inlet was tested in a 16-ft supersonic wind tunnel. The test article included the inlet

control actuators and the AIC. The bypass door control system could be tested in a closed-loop fashion, because the test article included the  $P_{ST}$  and  $P_{TT}$  throat sensors. The freestream  $P_{TO}$  and  $P_0$  probes were not available, because the aircraft forebody simulation did not include the location of the probes.

The inlet control systems operated properly and the bypass control system was stable.

The AIC used in this test and the AICs used in the first few flight test aircraft had programmable read only memories (PROM). Several modifications to the control system schedules were investigated during the wind tunnel testing by changing PROM constants in the AIC. In addition, some of the program constants had to be changed because simulated  $P_{TO}$  and  $P_0$  were used instead of data from probes. The digital mechanization again allowed rapid changing of program constants.

### Flight Testing and Performance Demonstration Results

This section presents some of the results obtained in flight and some of the problems encountered.

#### Air Inlet Controller Modifications During the Flight Test Program

After the full-scale inlet wind tunnel testing and a short ground test using the inlet controller stability and performance test rig, the inlet control system was flight tested. Several modifications were made in the AIC during the flight test program. Most of these were accomplished by reprogramming the AIC by means of the PROM chips in the AIC. The use of the PROM allowed rapid turnaround and minimized flight test delays. Since the changes were made in the AIC program, there was no need to perform the environmental requalification tests (shock, vibration, etc.) that are often required when discrete components such as resistors and capacitors are added to the circuit in analog mechanizations.

#### Excessive First Ramp Movement

Early in the flight test program, the pilots reported that the first ramp occasionally made abrupt movements, resulting in objectionable "thumping" and "banging" noises. The inlet controller stability and performance test rig was used to evaluate possible solutions to this problem. Based on these ground tests, a combination of fixes was devised. First, the forward loop gain of the first ramp control system was reduced 10%. Second, the AIC had been designed with a digital first-order lead in the angle-of-attack signal path, which had a time constant of 0.04 s. The lead was originally in the program to compensate for the delay caused by the dynamics of the angle-of-attack probe. The ground testing indicated that elimination of this lead would reduce the "thumping" problem. The third required fix was to place a second-order lag filter on the first ramp D/A converter output to smooth the output. The natural frequency of the filter is 120 rad/s. These fixes were installed, eliminating most of the "thumping" and "banging" noises.

In the months subsequent to the preceding modification, flight test personnel reported that the first ramp, at subsonic speeds, still appeared to be more active than necessary. At subsonic speeds, ramp motion is required mainly for improved aircraft stability requirements, which can be met with  $\frac{1}{2}$  of the fast response necessary to meet supersonic propulsion and airload requirements. Therefore, the AIC software was reprogrammed to reduce the AIC first ramp forward loop gain at subsonic speeds to  $\frac{1}{2}$  of the gain required at supersonic speeds. This eliminated first ramp motion complaints.

#### AIC Schedule Modifications

During the F-15 flight test program, the angle-of-attack probe and freestream pitot static probe corrections were

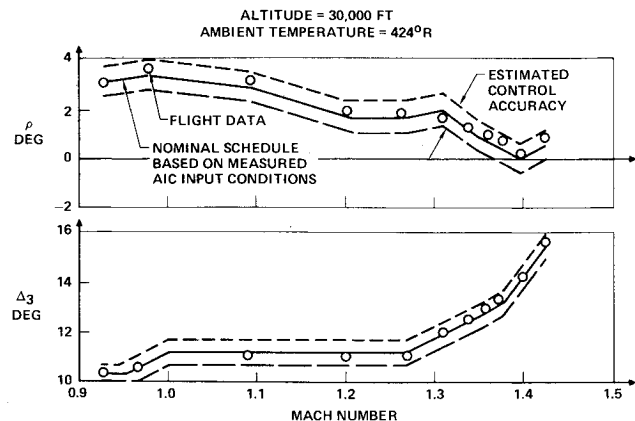


Fig. 10 Inlet ramp position comparison.

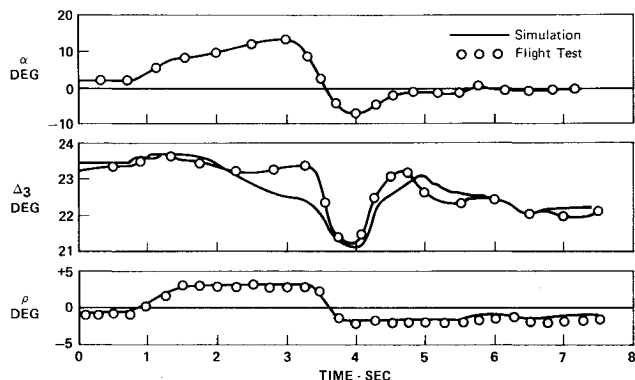


Fig. 11 Comparison of flight test and simulation response to pullup/pushover maneuver.

determined by comparison with measurements made with a noseboom and trailing cone probe. Two reprogrammings of the AIC were required during the flight test program, in order to change the pitot static and angle-of-attack probe correction factors and to modify the AIC schedules to match changes in the F-15 engine.

#### Air Inlet Control System In-Flight Accuracy

The in-flight accuracy of the first and diffuser ramp positioning is shown in Fig. 10. The flight measured data are shown by the circles. The nominal scheduled angles of the first and third ramps are also shown. The scheduled values are computed using the  $P_0$ ,  $P_{70}$ , and  $\alpha$  values measured by the AIC sensors. This eliminates the errors between noseboom and local measured values. As can be seen from Fig. 10, the ramps are positioned well within the allowable error bands. This indicates that the AIC is also well within the allowable accuracy limits.

#### Air Inlet Control System Dynamic Response Testing

A rapid aircraft pullup followed by a rapid pushover was used to demonstrate the dynamic response capability of the air inlet control system. The transient was performed near Mach 2.3 at 50,000 ft, which is one of the more sensitive flight conditions in terms of engine/inlet stability dependence upon accuracy of inlet ramp positioning. The aircraft angle of attack, first ramp angle, and third ramp angle are shown in Fig. 11 as a function of time. This is one of the more extreme maneuvers that will be seen by the inlet. It can be seen from Fig. 11 that the angle-of-attack rate is greater than 30 deg/s. All of the AIC inputs were determined from the flight test data and were input to the dynamic simulation used for design purposes. The response of the simulation is also shown in Fig. 11. There is good agreement between flight test and simulation results for the first and third ramp control systems. The control system errors did not cause supercritical or buzz operation of the inlet, and did not cause excessive decrease in the inlet performance. These results indicate that the inlet control system component dynamic errors are not excessive.

#### Conclusions

Early design study results indicated that desired F-15 performance could be achieved with an engine air inlet controlled as a function of Mach number, freestream total temperature, and angle of attack. A subsequent trade study showed that a serial digital mechanization of the AIC would provide the best implementation of the AIC electronics required to control this engine air inlet. The results of this latter study were corroborated by the excellent performance demonstrated with the digital system during the flight test program. The dynamic response requirements of the AIC were chosen based on studies using a simulation of the engine air inlet system. The results obtained during the ground and flight testing indicated that the AIC sample rates chosen are adequate for this application. Comparison of the dynamic simulation and in-flight time responses showed close agreement, indicating that the simulation was a good design tool.

The capability of the AIC for meeting the specified accuracy requirement was fully demonstrated during flight testing. The successful in-flight operation of the F-15 weapon system in meeting its performance and mission goals indicates the success of this inlet control concept using a serial digital computer AIC mechanization.

#### References

- <sup>1</sup>Sams, "F-15 Propulsion System Design and Development," AIAA Paper 75-1042, Los Angeles, Calif., Aug. 1975.
- <sup>2</sup>Imfeld, W.F., "The Development Program for the F-15 Inlet," AIAA Paper 74-1061, San Diego, Calif., Oct. 1974.
- <sup>3</sup>Mello, J.F., "Testing for Design - F-15 Powerplant Integration," AIAA Paper 75-328, Washington, D.C., Feb. 1975.